



Development of WC-Co Coatings Deposited by Warm Spray Process

Pornthep Chivavibul, Makoto Watanabe, Seiji Kuroda, Jin Kawakita, Masayuki Komatsu, Kazuto Sato, and Junya Kitamura

(Submitted June 24, 2008; in revised form September 19, 2008)

The high-velocity oxy-fuel (HVOF) process is commonly used to deposit WC-Co coatings. There are some problems with this process; especially the decomposition and decarburization of WC during spraying make a coating brittle. To suppress such degradation, the warm spray (WS) process was applied to deposit WC-Co coatings, which is capable of controlling the flame temperature in the range of 500–2000 °C. The microstructure and phases of the deposited coatings were characterized by using SEM and XRD, and the mechanical properties such as hardness, fracture toughness, and wear properties were also investigated. WS process successfully suppressed the formation of the detrimental phases such as W₂C and W, which are usually observed in HVOF coatings. The WS coatings showed the similar trend of the hardness variation for Co content with a sintered bulk material. Improvement of toughness and wear behavior was also observed in WS coatings.

Keywords coating, HVOF, warm spray, WC-Co

1. Introduction

WC-Co cermet coatings have been used to enhance the wear resistance of various engineering components in a variety of industrial environments. Many thermal spraying techniques, such as atmospheric plasma spraying (APS) and high-velocity oxy-fuel (HVOF) spraying, can be applied to deposit WC-Co coatings; however, the properties of such coatings strongly depend on the spraying technique. Compared to other spraying techniques, HVOF spraying is one of the best methods for depositing conventional WC-Co cermets, because the higher velocities and lower temperatures experienced by the powder results in less decomposition of the WC during spraying (Ref 1). Therefore, coatings with higher amount of retained WC and lower porosity are expected. However, when compared to sintered bulk WC-Co, for which the

sintering atmosphere has been carefully controlled, HVOF-sprayed WC-Co coatings suffer from decomposition and decarburization during spraying process leading to a formation of undesirable phases such as W₂C, W, and amorphous or nanocrystalline Co-W-C phase (Ref 2, 3). Many studies have shown the effects of these phases on the properties of the coating (Ref 3–7). Chivavibul et al. (Ref 5) systematically studied the effects of both carbide size and Co content on the mechanical properties of the coatings. They found that the hardness and fracture resistance behaviors of the coating were different from those of the bulk materials. This discrepancy could be explained by the hardening of the binder phase due to the dissolution of WC and the formation of amorphous/nanocrystalline phases. The hardness of the binder phase estimated from the experimental data was ranged from 1000 to 1300 Hv, and significantly higher than that of the bulk binder phase (490–660 Hv).

Many efforts have been made to deposit WC-Co coatings at lower process temperature than HVOF to suppress decarburization and decomposition of WC phases (Ref 8–14). Jacob et al. successfully deposited WC-Co and WC-Co-Cr coatings using high-velocity air fuel (HVOF) process (Ref 12, 13). These coatings showed no detrimental phase from decomposition or oxidation during deposition. Compared to HVOF coatings, the HVOF WC-Co-Cr coating showed the improved hardness and wear resistance. On the other hand, HVOF WC-Co coating showed lower hardness than HVOF and there was no comparative result of wear property. Recently, the success in using cold spray technique to deposit various metallic materials (Ref 15, 16) has invoked a great interest to apply this technique to deposit WC-Co coatings. The earlier work by Lima et al. (Ref 8) showed that the nano WC-Co coatings could be deposited, but the thickness of the coating was less than 10 μm. The nano WC-Co

This article is an invited paper selected from presentations at the 2008 International Thermal Spray Conference and has been expanded from the original presentation. It is simultaneously published in *Thermal Spray Crossing Borders, Proceedings of the 2008 International Thermal Spray Conference*, Maastricht, The Netherlands, June 2–4, 2008, Basil R. Marple, Margaret M. Hyland, Yuk-Chiu Lau, Chang-Jiu Li, Rogerio S. Lima, and Ghislain Montavon, Ed., ASM International, Materials Park, OH, 2008.

Pornthep Chivavibul, Makoto Watanabe, Seiji Kuroda, Jin Kawakita and Masayuki Komatsu, Composites and Coatings Center, National Institute for Materials Science, Ibaraki, Japan; and **Kazuto Sato and Junya Kitamura**, Fujimi Incorporated, Gifu, Japan. Contact e-mail: Watanabe.Makoto@nims.go.jp.

coatings with thickness over 100 μm were successfully deposited by Kim et al. (Ref 9, 10) and Li et al. (Ref 14). These coatings have extremely high hardness (1820–2050 Hv) and show no detrimental phase formation in the coatings. Although the overall performances of these coatings such as toughness and wear properties are still unknown, it indicates the capability of cold spray to fabricate WC-Co coatings, which have a similar microstructure as the sintered bulk materials.

Kawakita et al. (Ref 17, 18) has developed a new process named *warm spray* process (WS). This process has a mixing chamber between the combustion chamber and the powder feed ports. The combustion is generated within the chamber and then it is mixed with nitrogen to control the temperature of the gas. Compared to the cold spray deposition, this technique provides a capability to control the temperature of sprayed particles in a wide range. The success of using this technique to deposit various materials (Ref 17–20) such as titanium and metallic glass has been reported. Recently, Watanabe et al. (Ref 11, 18) demonstrated a capability of this technique to deposit WC-12Co coating. The coating showed no detrimental phases and had the same level of hardness as the sintered bulk material and HVOF coating of the same composition. However, the systematic study of this process is still required on the application of WC-Co coatings.

In the present investigation, a comparative study of WS and HVOF coatings is performed to verify the capability of WS process as a new candidate for cermet coating. The nano-sized WC-Co powders with various Co contents were sprayed by both WS and HVOF techniques. Phase distribution and microstructure of the coatings were examined by X-ray diffraction and scanning electron microscope (SEM), respectively. Hardness, fracture toughness, and abrasive wear properties were measured. The relation between the microstructural features and the mechanical properties are discussed based on the experimental results.

2. Experimental Procedure

2.1 Materials and Spraying Process

Three commercially available WC-Co powders with an average carbide size of 0.2 μm and different cobalt contents (12, 17, and 25 wt.%) were used in this work. The powders were manufactured by spray drying of slurries containing WC and Co particles, followed by light sintering, crushing, and classification. The particle size of the powders ranged from 15 to 45 μm . Examples of the morphology and cross section of WC-12Co and WC-25Co powder are shown in Fig. 1. All powders have typically spherical shape. The WC-12Co powder shows dense packing of fine carbide, while WC-25Co powder shows more loosely packed structure with higher amount of pores. The Co distribution in all the powder is not uniform. Many Co pools can be clearly observed in WC-25Co powder.

A commercial HVOF spraying equipment (JP5000, Praxair Technology Inc., USA) was used to spray these powders onto carbon steel (0.45% C) substrates. The WS process was performed by adding the mixing chamber between the combustion chamber and powder feed port of the HVOF equipment. Details of the spraying equipment were given elsewhere (Ref 17, 18). Table 1 shows the spraying conditions of HVOF and WS processes. The thickness of the coatings was approximately 300 μm .

2.2 Coating Characterization

X-ray diffraction (XRD) was conducted for the powders and as-fabricated coatings with Cu $K\alpha$ radiation at 40 kV and 300 mA. Cross sections of the coatings were obtained by embedding a specimen in cold-mounting resin followed by grinding and polishing to a 1 μm finish and examined by scanning electron microscopy (SEM).

Microhardness tests were carried out with a 300 g load and a dwell time of 15 s. At least ten measurements were made for each sample. The fracture toughness of the coatings was determined by the indentation method with a 10 kg load and a dwell time of 15 s. Both the crack lengths and Vickers diagonals were measured by an optical microscope. The fracture toughness, K_{IC} , was determined under an assumption that the cracks generated from an indentation were radial cracks possessing the Palmqvist geometry by the following equation (Ref 21):

$$K_{IC} = 0.0193(H_v D)^{2/5} (a)^{-1/2}, \quad (\text{Eq 1})$$

where H_v is the Vickers hardness, E is the Young's modulus, D is the half-diagonal of the Vickers indentation, and a is the indentation crack length. At least five indentations were made for each sample. The Young's modulus of the coatings was assumed to be 300 GPa for all the samples.

Abrasive wear of the coatings was evaluated using a Suga-type wear tester (two-body abrasive wear tester). The test was performed by the reciprocating motion of the test specimen scratching on a rotating wheel under a load of 29.4 N. The wheel had a diameter of 50 mm and was covered with 180 mesh SiC paper ($\sim 78 \mu\text{m}$). To eliminate the effect of surface condition, all test specimens were polished before the test. The weight loss of the test specimen was measured after each run of 400 cycles, which corresponds to 25.6 m sliding distance, and the tests were performed up to three runs for each specimen. The average weight losses of all the samples were converted to volume losses by using density values of the bulk materials and then normalized with that of the JIS-SS400 carbon steel.

3. Results and Discussion

3.1 Coating Microstructure

Examples of BSE images of HVOF and WS coatings are shown in Fig. 2. The image of HVOF and WS WC-12Co are shown in Fig. 2(a) and (b), respectively. Both revealed a dispersion of fine carbide particles in binder

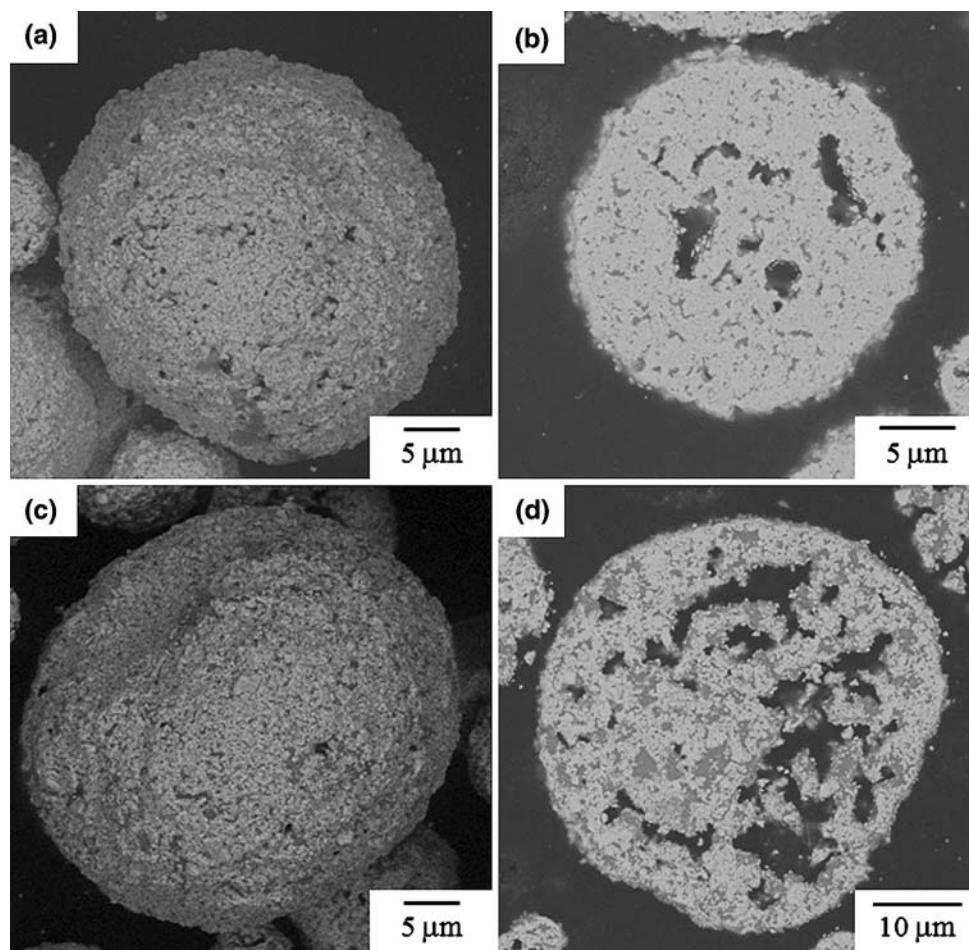


Fig. 1 SEM observation of powders (a), (b) WC-12Co and its cross section, (c) and (d) WC-25Co and its cross section

Table 1 Spray conditions for WC-Co coatings

	WS	HVOF
Barrel length, mm	203	152
Spraying distance, mm	200	380
Fuel, L/min	0.38	0.38
Oxygen, L/min	778	944
Nitrogen, L/min	500	...
Powder feed rate, g/min	80	80
Powder feed gas	Nitrogen	Nitrogen

layers. Pores were observed in both coatings. In some area of the HVOF WC-12Co coatings, lack of splat-splat bonding was also observed as shown in Fig. 2(a). A clear difference of microstructure between HVOF and WS coating can be observed in coating with higher Co content. The HVOF WC-25Co coating (Fig. 2c) showed carbides distribution in binder layers with different contrasts. These bright and dark binder layers were W-rich and Co-rich regions, respectively. The bright binder layer was not observed in the WS WC-25Co coating (Fig. 2d). Moreover, the carbide fractions in HVOF coatings were much lower than those in WS coatings. The shape of carbides in HVOF coating became rounder than that of WS coatings.

The loss of carbide and change of carbide morphology in HVOF coatings could be attributed to the dissolution of WC into the Co binder, while such reaction can be suppressed by WS process. This process provides a deposition of feedstock powder in solid state, therefore the microstructure of the coating results from the stacking of particles under impact. This means that the microstructure of the starting powder strongly influences the coating microstructure. This can be confirmed by comparing the cross sections of WC-25Co powder (Fig. 1d) to that of the coating (Fig. 2b). Co pools could be observed in both the powder and the coating.

Examples of XRD patterns of HVOF and WS coatings are shown in Fig. 3(a) and (b), respectively. The results of WC-12Co feedstock powder is also given for a comparison. While the original powder contained only the peaks of Co and WC, HVOF coatings showed the crystalline peaks of WC, W₂C, W, and a broad shoulder at the angle of the Co peak, indicating that the binder has attained amorphous or nanocrystalline form. There is a tendency for amorphous peak to increase as the Co content increases, while W₂C tended to decrease. In the case of WS coatings, only the peaks of WC and Co phase can be clearly recognized for the 17 and 25% Co contents, while a

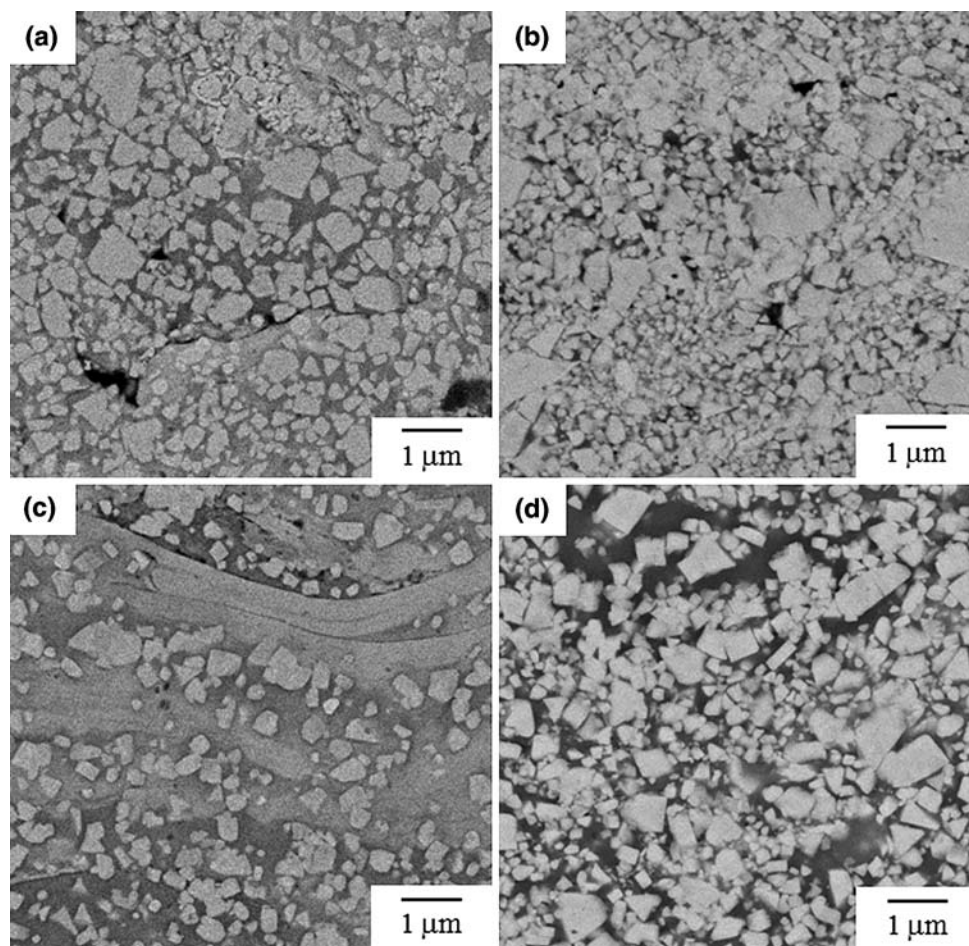


Fig. 2 SEM observations of (a) HVOF WC-12Co, (b) WS WC-12Co, (c) HVOF WC-25Co, and (d) WS WC-25Co coatings

very small peak of W_2C is observed in the 12% Co content. This meant that WS process can significantly suppress the decomposition and oxidation during deposition. However, it was noted from Fig. 2(b) that the Co peaks were broadened and shifted to lower angles. One possible explanation can be the deformation of Co phases due to high-velocity impact of particle during deposition. Large deformation of soft Co binder and constraining by the surrounding carbides can generate high residual compressive stress in the binder, and thus only the Co peak shows a substantial peak shift. For broadening of the peak, since the high-speed impact of solid particle induces the dynamic recrystallization and leads to the formation of nano-order polycrystalline structure (Ref 22), the formation of such nanocrystalline microstructure possibly occurred in the coatings.

3.2 Mechanical Properties of the Coating

The microhardness and fracture toughness values of the HVOF and WS coatings, as a function of Co content, are shown in Fig. 4. The values of a sintered bulk material are also given for a comparison (Ref 23). Generally, the hardness of a bulk material decreases with increasing cobalt

content. The hardness of both HVOF and WS coatings also decreased with increasing Co content, but the gradients of the trend lines reveal clear difference between them. While the WS coatings had softer than the bulk for all Co contents, a trend of hardness variation was similar to the bulk. In contrast, the hardness of HVOF coatings only shows slight variation with Co content and the gradient of the line was quite different with the ones of the bulk and WS coatings. Based on the XRD results, the HVOF coatings contained new phases such as W_2C , W, and amorphous or nanocrystalline binder phase. Although the WC contents in HVOF coatings were lower than those in the bulk and WS coatings (e.g., Fig. 2d), the formation of such new phases affected the hardness significantly. The hardness of W_2C and amorphous binder are reported to be approximately 3000 and 1000-1300 Hv, respectively, which are higher than WC (Hv = 1300-2300) and Co binder (Hv = 490-660) (Ref 5). While the hardness of the bulk material and the WS coatings depends on the amount of WC content, one of the HVOF coatings depends more on the properties of binder resulting in relatively small variation for Co content.

When the data of WS coatings is compared with the bulk, it shows 10-20% lower values for 12-25% Co content. This may be due to the existence of the microstructural

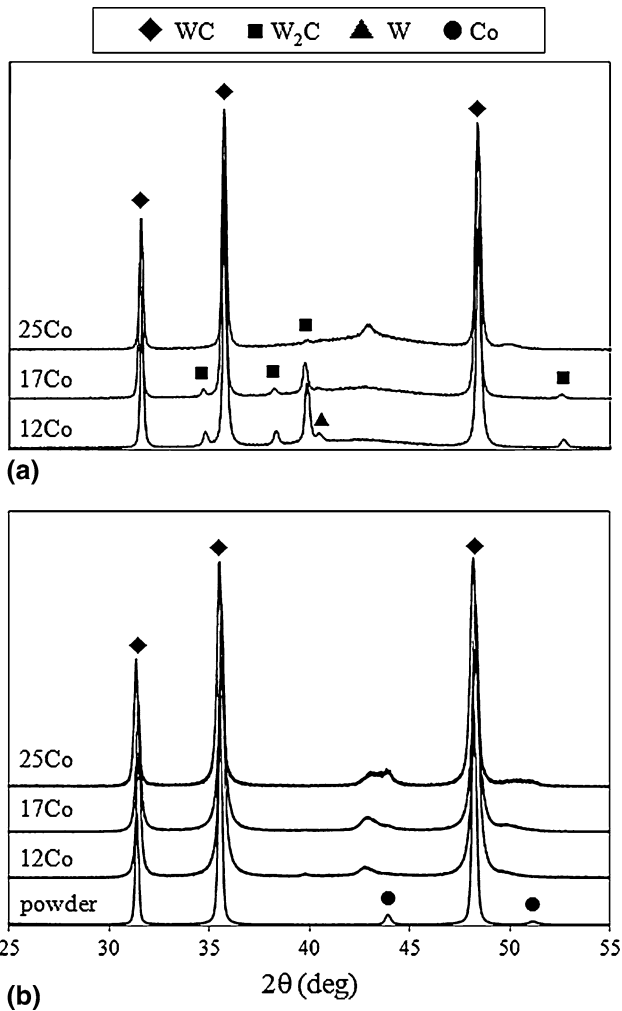


Fig. 3 XRD results of (a) HVOF and (b) WS coatings. The result of WC-12Co powder coatings is given for a comparison

defects such as pores, which can be recognized in Fig. 2(b) as black dots. Although the adhesion mechanism of a WC-Co particle in WS deposition is yet to be studied, it is hypothesized that Co binder would work as a kind of glue with significant deformation upon impact. Thus, if there were not enough amounts of Co on the surface of a particle locally, for example, due to nonuniform distribution of Co in one particle, those regions could be poorly bonded. More detail experiments are required to minimize the gap between a bulk material and a WS coating.

In Fig. 4, the fracture toughness of both HVOF and WS coatings ranged from 4 to 6 MPam^{1/2}. Figure 5 shows the cross-sectional images of the crack configurations in WC-17Co coatings after the test deposited by (a) HVOF and (b) WS, respectively. The drastic reduction in crack length can be recognized in WS sample indicating the effectiveness of suppression of the formation of brittle W₂C and amorphous binder phases for crack resistance. These values, however, are still lower than those of bulk WC-Co (9-14 MPam^{1/2}). Figure 6(a) shows SEM photograph of the crack path generated from indentation test of HVOF

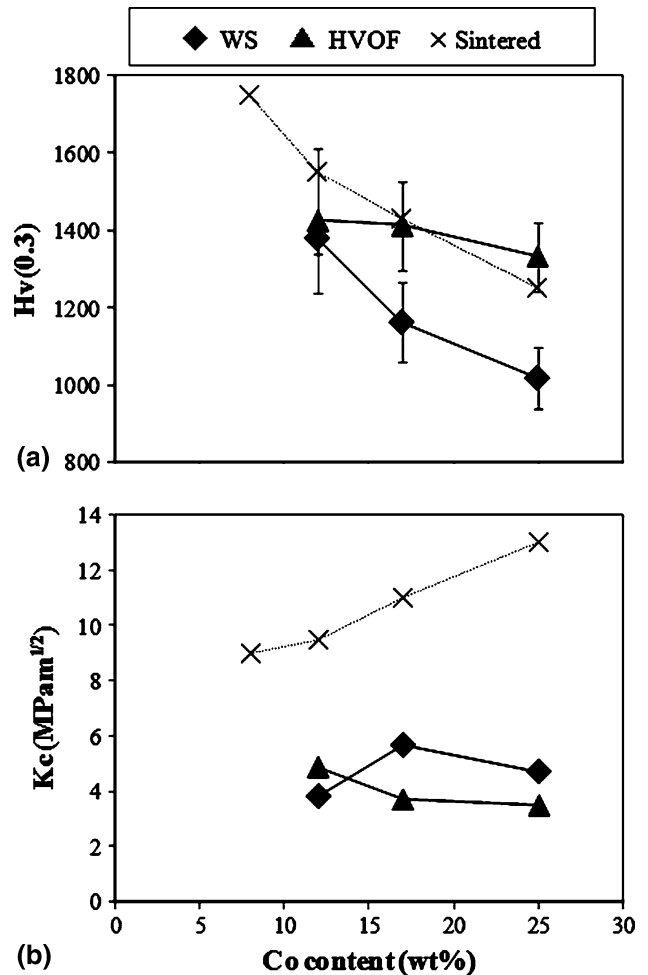


Fig. 4 (a) Hardness and (b) fracture resistance as a function of cobalt content. Values of the sintered materials were given for a comparison (Ref 23)

WC-25Co coating. The crack preferentially propagated through the W-rich binder regions (white-colored area) indicating lower fracture toughness of these regions. This observation showed that the microstructure of the binder plays an important role in the mechanical properties of the HVOF coatings. Although WS coatings showed no changes in phase composition as mentioned in previous section, the increase of toughness with increasing Co content in WS coatings was very small as compared with bulk materials. This might be attributed to their inhomogeneous microstructure. Figure 6(b) shows SEM photograph of the crack path generated from fracture toughness indentation test of WS WC-25Co coating. In contrast to the HVOF coating, crack propagated through the WC-WC interface and the region which might be splat-splat boundary. Another point noted from Fig. 6(b) is that there are Co pools in the coating indicating the poor distribution of Co content. This also gave an effect on the fracture toughness properties by causing nonuniform stress distribution.

Abrasive wear behaviors of HVOF and WS coatings as a function of Co content are shown in Fig. 7. To avoid any

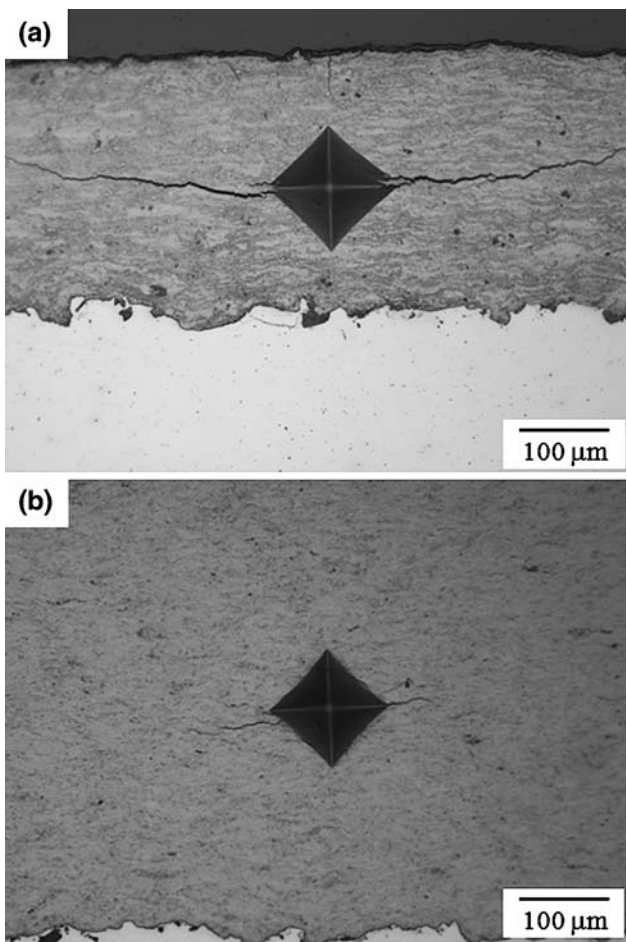


Fig. 5 Cracks generated by the indentation fracture toughness test (load: 10 kgf) in WC-17Co coatings by (a) HVOF and (b) WS depositions. Drastic reduction of crack length can be recognized in the WS coating

effect of variation in the quality of SiC paper from different lots, data were presented as volume loss normalized with that obtained from JIS-SS400 steel. The volume wear loss increased with increasing Co content in both HVOF and WS coatings. The WS WC-12Co coatings showed great improvement of wear property compared to the HVOF one; however, higher volume wear losses were observed in the coatings with higher Co contents. This behavior was related to the phase distribution and microstructure of the coatings. Considering WC-12Co, HVOF and WS coatings showed the same hardness value while XRD results of HVOF coatings showed higher amount of W_2C and W. These brittle phases and the amount of defects in HVOF coatings lead to higher wear volume loss than that observed in WS coating. For higher Co contents, WS coatings contain a number of Co pools (Fig. 2d and 6b) while the binder phases in the HVOF were hardened by the dissolution and decarburization of WC (Fig. 2c and 6a). Such Co pools in WS coatings, presumably softer than the binder in HVOF coatings, could be preferentially removed during the wear test. This may

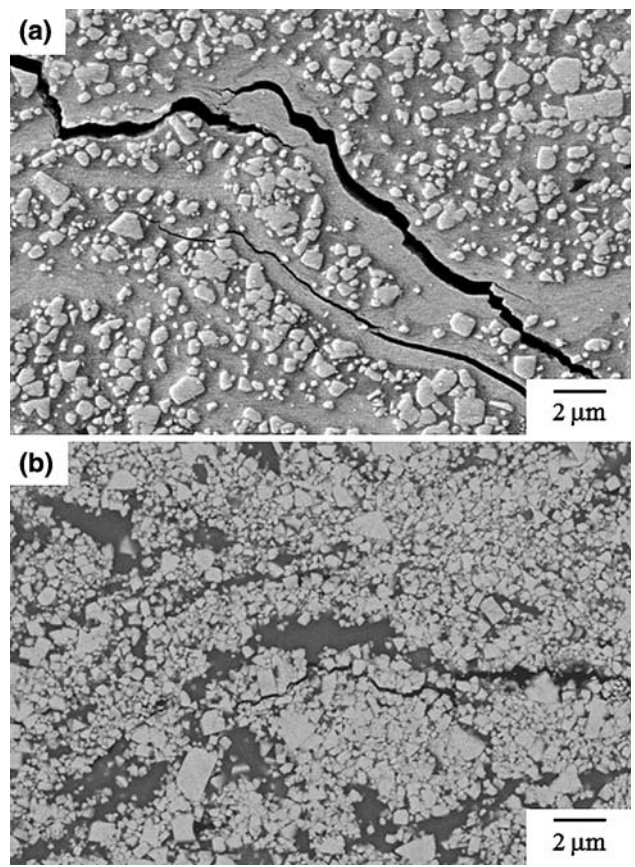


Fig. 6 SEM observation of cracks generated from fracture toughness test of WC-25Co deposited by (a) HVOF and (b) WS techniques. Arrows indicate the region which might be splat-splat boundary

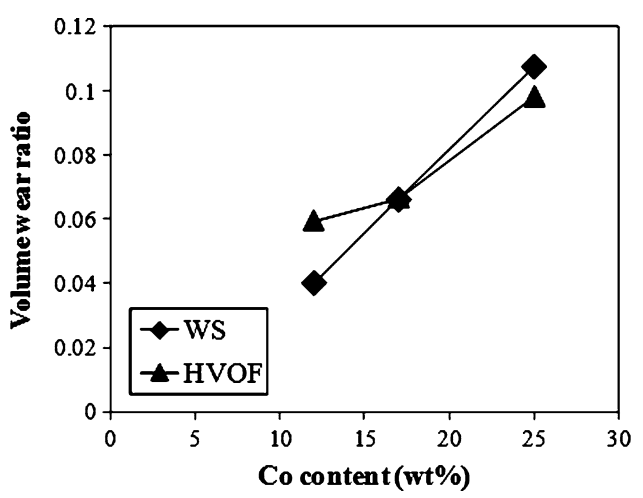


Fig. 7 Suga wear ratio as a function of Co content

be a reason for higher wear loss for 25% Co in WS coatings compared to HVOF ones. A plot of reciprocal of volume wear ratio as a function of coating hardness is shown in Fig. 8. The reciprocal volume wear ratio was

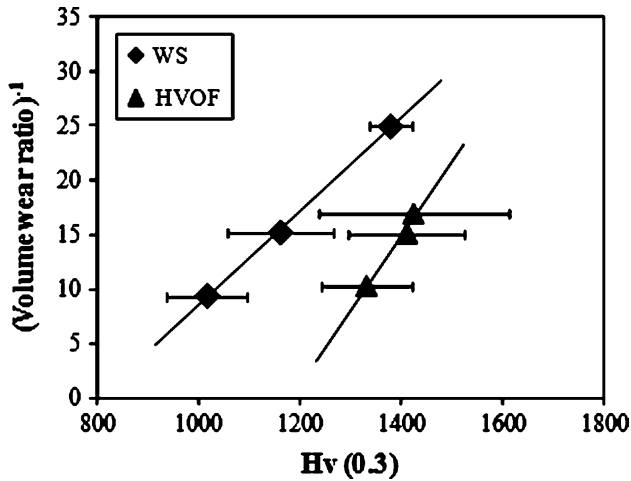


Fig. 8 Reciprocal of Suga wear ratio as a function of coating hardness

chosen because it likely shows the influence of hardness in a linear fashion. Fitting curves showed good linear relation for both HVOF and WS coatings. For a given hardness value, WS coating showed better wear performance than HVOF coating. This improvement was related to the microstructure and phase distribution of the WS coating. One important factor was the difference of binder properties between HVOF and WS coatings. Detailed studies for further improvement in mechanical properties of WS coatings are required.

4. Conclusions

WC-Co coatings with 0.2 μm carbide size and different cobalt contents were obtained by HVOF and warm spraying of three commercial powders. The microstructure, hardness, fracture toughness, and wear behavior of the coatings were investigated.

Characterization of the coatings revealed different mechanical properties between WS and HVOF coatings. The hardness-Co content relation in WS coatings was similar to that in sintered bulk materials, while different behavior was observed in HVOF coatings. Fracture toughness tended to increase with increasing Co content in WS coatings, while HVOF coatings showed the opposite trend. The improvement in wear property was also observed in WS coatings. These could be explained by the microstructure and phase distribution in the coating. The WS technique showed capability to deposit WC-Co coating without dissolution and decarburization of WC.

References

- V.V. Sobolev, J.M. Guilemany, and J. Nutting, *High Velocity Oxy-Fuel Spraying*. Maney Publishing, UK, 2004
- J.M. Guilemany, J.M. de Paco, J. Nutting, and J.R. Miguel, Characterization of the W₂c Phase Formed During the High Velocity Oxygen Fuel Spraying of a Wc+12 Pct Co Powder, *Metall. Mater. Trans. A*, 1999, **30**(8), p 1913-1921
- C. Verdon, A. Karimi, and J.L. Martin, A Study of High Velocity Oxy-Fuel Thermally Sprayed Tungsten Carbide Based Coatings. Part 1: Microstructures, *Mater. Sci. Eng. A*, 1998, **246**(1-2), p 11-24
- Y. Ishikawa, J. Kawakita, S. Sawa, T. Itsukaichi, Y. Sakamoto, M. Takaya, and S. Kuroda, Evaluation of Corrosion and Wear Resistance of Hard Cermet Coatings Sprayed by Using an Improved HVOF Process, *J. Therm. Spray Technol.*, 2005, **14**(3), p 384-390
- P. Chivavibul, M. Watanabe, S. Kuroda, and K. Shinoda, Effects of Carbide Size and Co Content on the Microstructure and Mechanical Properties of HVOF-Sprayed WC-Co Coatings, *Surf. Coat. Technol.*, 2007, **202**(3), p 509-521
- M. Watanabe, A. Owada, S. Kuroda, and Y. Gotoh, Effect of Wc Size on Interface Fracture Toughness of WC-Co HVOF Sprayed Coatings, *Surf. Coat. Technol.*, 2006, **201**(3-4), p 619-627
- Y. Ishikawa, S. Kuroda, J. Kawakita, Y. Sakamoto, and M. Takaya, Sliding Wear Properties of HVOF Sprayed WC-20%Cr3c2-7%Ni Cermet Coatings, *Surf. Coat. Technol.*, 2007, **201**(8), p 4718-4727
- R.S. Lima, J. Karthikeyan, C.M. Kay, J. Lindemann, and C.C. Berndt, Microstructural Characteristics of Cold-Sprayed Nanostructured WC-Co Coatings, *Thin Solid Films*, 2002, **416**(1-2), p 129-135
- H.J. Kim, C.H. Lee, and S.Y. Hwang, Superhard Nano WC-12%Co Coating by Cold Spray Deposition, *Mater. Sci. Eng. A*, 2005, **391**(1-2), p 243-248
- H.J. Kim, C.H. Lee, and S.Y. Hwang, Fabrication of WC-Co Coatings by Cold Spray Deposition, *Surf. Coat. Technol.*, 2005, **191**(2-3), p 335-340
- M. Watanabe, C. Pornthep, S. Kuroda, J. Kawakita, J. Kitamura, and K. Sato, Development of WC-Co Coatings by Warm Spray Deposition for Resource Savings of Tungsten, *J. Jpn. Inst. Metals*, 2007, **71**, p 853-859
- L. Jacobs, M.M. Hyland, and M. De Bonte, Comparative Study of WC-Cermet Coatings Sprayed via the HVOF and the HVOF Process, *J. Therm. Spray Technol.*, 1998, **7**(2), p 213-218
- L. Jacobs, M.M. Hyland, and M. De Bonte, Study of the Influence of Microstructural Properties on the Sliding-Wear Behavior of HVOF and HVOF Sprayed WC-Cermet Coatings, *J. Therm. Spray Technol.*, 1999, **8**(1), p 125-132
- C.J. Li, G.J. Yang, P.H. Gao, J. Ma, Y.Y. Wang, and C.X. Li, Characterization of Nanostructured WC-Co Deposited by Cold Spraying, *J. Therm. Spray Technol.*, 2007, **16**, p 1011-1020
- L. Ajdelsztajn, B. Jodoin, and J.M. Schoenung, Synthesis and Mechanical Properties of Nanocrystalline Ni Coatings Produced by Cold Gas Dynamic Spraying, *Surf. Coat. Technol.*, 2006, **201**(3-4), p 1166-1172
- T.H. Van Steenkiste, J.R. Smith, and R.E. Teets, Aluminum Coatings via Kinetic Spray with Relatively Large Powder Particles, *Surf. Coat. Technol.*, 2002, **154**(2-3), p 237-252
- J. Kawakita, S. Kuroda, T. Fukushima, H. Katanoda, K. Matsuo, and H. Fukunuma, Dense Titanium Coatings by Modified HVOF Spraying, *Surf. Coat. Technol.*, 2006, **201**(3-4), p 1250-1255
- S. Kuroda, J. Kawakita, M. Watanabe, and H. Katanoda, Warm Spraying—A Novel Coating Process Based on High-Velocity Impact of Solid Particles, *Sci. Technol. Adv. Mater.*, 2008, **9**(3), p 033002
- J. Kawakita, S. Kuroda, S. Krebs, and H. Katanoda, In-Situ Densification of Ti Coatings by the Warm Spray (Two-Stage HVOF) Process, *Mater. Trans.*, 2006, **47**(7), p 1631-1637
- J. Kawakita, N. Maruyama, S. Kuroda, S. Hiromoto, and A. Yamamoto, Fabrication and Mechanical Properties of Composite Structure by Warm Spraying of Zr-Base Metallic Glass, *Mater. Trans.*, 2008, **49**(2), p 317-323
- M.M. Lima, C. Godoy, J.C. Avelar-Batista, and P.J. Modenesi, Toughness Evaluation of HVOF WC-Co Coatings Using Non-Linear Regression Analysis, *Mater. Sci. Eng. A*, 2003, **357**(1-2), p 337-345
- K. Kim, M. Watanabe, J. Kawakita, and S. Kuroda, Grain Refinement in a Single Titanium Powder Particle Impacted at High Velocity, *Scr. Mater.*, 2008, **59**(7), p 768-771
- G.S. Upadhyaya, *Cemented Tungsten Carbides: Production, Properties, and Testing*. Noyes Publications, Westwood, NJ, 1998